Effect of Heat Treatment on the Microstructure of a Metastable β-Titanium Alloy

X. Huang, J. Cuddy, N. Goel, and N.L. Richards

Metastable β-titanium alloys have improved formability and ductility compared to high-strength α- and α+β titanium alloys; this can be attributed to their body-centered cubic structure in the solution-treated condition. In addition, a high strength level can be achieved by a simple aging treatment. During manufacturing, components are subjected to a variety of thermal cycles at temperatures ranging from 650 to 925 °C, as well as to cooling rates that vary from air cooling to furnace cooling. Consequently, various microstructures are produced that influence the mechanical properties of the products. The present study was undertaken to characterize the precipitation behavior of Timetal 21S at various heat treatment conditions by employing x-ray diffraction techniques combined with optical and scanning electron microscopy. It was observed that α precipitated preferentially on the grain boundaries during high-temperature aging (650 °C) and within the grains during low-temperature aging (400 °C). High-temperature solutioning produced a coarse grain size, and at the same time enhanced finer α precipitation during aging. The amount of α precipitate attained after the standard aging treatment was about 33%. Re-solution treatment followed by slow cooling, such as that which occurred during brazing of the alloy, resulted in α precipitation during cooling; however, an aging treatment was necessary to precipitate an α content greater than 20%.

Keywords

β-Ti, brazing, heat treatment, microstructure, precipitation, titanium alloys, x-ray diffraction

1. Introduction

TIMETAL 21S is a metastable β-titanium alloy that appears to be a promising candidate for aerospace applications because of its formability, elevated-temperature properties, low density, and oxidation resistance. The alloy was developed at TIMET, Denver, CO, in the late 1980s, to overcome various shortcomings of other titanium alloys, such as the poor formability of α+β alloys and the reduced elevated-temperature properties of β alloys. After extensive screening by the manufacturer, the composition was selected as Ti-15Mo-2.7Nb-3Al-0.2Si-0.15O_2 and was designated β-21S (meaning a β alloy that contains 21% alloying additions and Si) (Ref 1). Alloy 21S has subsequently been renamed Timetal 21S by the manufacturer. Timetal 21S has been shown to be highly oxidation resistant compared to commercially pure titanium and other β alloys (such as Ti-15-3) (Ref 1, 2). In the aged condition, the material shows very good stability up to 538 °C, with minor change in strength and no loss in ductility (Ref 1). Timetal 21S has also been characterized as having resistance to hot, reducing acid environments equivalent to that of grade 7 titanium (Ref 3). As a metastable β alloy, Timetal 21S is readily age hardened by heat treating at 482 °C to 593 °C for various amounts of time to achieve peak hardness.

The physical and mechanical properties of Timetal 21S have been examined by several researchers (Ref 1-4); however, very limited information is available in the literature regarding its microstructural aspects. The present study was undertaken to investigate the microstructure of the alloy in three conditions: as received; aged; and re-solution treated during brazing, slowly cooled in the furnace, and subsequently aged.

X. Huang, J. Cuddy, N. Goel, and **N.L. Richards,** M & P Laboratories, Bristol Aerospace Ltd., Winnipeg, Canada

2. Experimental Procedures

The material used in this investigation was supplied by TIMET with a composition as given in Table 1. Specimens were heat treated according to the parameters listed in Table 2 in an air furnace, with the samples sealed in stainless steel bags. Microstructural examination and x-ray diffraction (XRD) were conducted on both as-received and heat-treated materials.

Samples for metallographic examination were prepared by the following standard sequences: sectioning, mounting, and mechanical polishing. Samples were etched by etching-polishing methods using γ-Al_2O_3 slurry and Kroll's reagent.

The specimens for XRD were first mechanically ground to remove the surface oxide and then etched in hydrofluoric acid to remove the deformation layer. The XRD analysis was conducted using a Philips (North American Philips Co., Williamsport, PA) PW1710 automated diffractometer system. The

Table 1 Chemical composition of as-received material

Composition, wt%							
Al	Mo	Si	Nb	Fe	C	N	O
3.15	14.4	0.19	2.56	0.32	0.012	0.016	0.014

Table 2 Heat treatment cycles

Solution temperature, °C	Time	Cooling rate	Aging temperature, °C	Time	α, % (determined by XRD)
AR*	...	...	...	...	...
AR	...	...	400	4 h	...
AR	...	...	400	8 h	...
AR	...	...	538	8 h	33
AR	...	...	677	1 h	0
AR	...	...	677	4 h	...
AR	...	...	677	8 h	...
816	1 h	22 °C/min	538	8 h	...
927	1 h	22 °C/min	...	...	...
927	1 h	22 °C/min	538	8 h	24
927	1 h	FC at 2 °C/min to 300 °C	...	...	13.5
927	1 h	FC at 2 °C/min to 538 °C AC	...	...	7.7
927	1 h	FC at 2 °C/min to 538 °C AC	538	8 h	25
927	1 h	FC at 2 °C/min to 593 °C AC	...	...	...
677 (ABTi)	40 min	6 °C/min	...	...	...
677 (ABTi)	40 min	6 °C/min	538	8 h	25

Note: ABTi, aluminum-brazed titanium; AC, air cool; AR, as received; FC, furnace cool. * The as received material was originally solution treated by supplier at a temperature between 810 and 843 °C.

Table 3 Lattice parameters of two phases present in β-21S

Phase	Lattice parameter
hcp α ($P_6(3)/MMC$)	$a = 2.9428$ A, $c = 4.680$ A
bcc β (I_m-3m)	$a = 3.2488$ A

equipment settings were 40 kV, 40 mA, 6° takeoff angle, a step interval of 0.05° 2θ, and a step counting time of 3 s. Structures for both α and β phases were refined with the DBWS-9006PC Rietveld program. The weight fractions of α and β phases were calculated based on the methods of Hill and Howard (Ref 5) using the following equation:

$$W_p = \frac{S_p(ZMV)_p}{\sum S_1(SMV)_i}$$

where S is the Rietveld scale factor, Z is the number of formula units per unit cell, M is the mass of the formula unit, V is the unit-cell volume, and p represents different phases.

Microstructural examination was carried out using both an optical microscope and a scanning electron microscope (SEM) (Jeol JXA850) equipped with a Tracor Northern energy-dispersive spectrometer (EDS).

3. Results

3.1 *X-Ray Diffraction*

The phase precipitated during aging was identified by XRD to be the α-hcp (hexagonal close-packed) phase with lattice parameters as shown in Table 3. The amounts of α precipitated after various heat treatments are shown in Table 2.

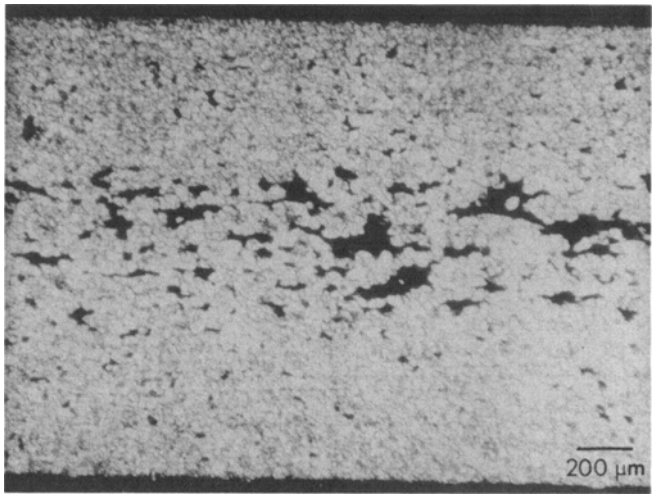

Fig. 1 Microstructure of as-received material

The amount of α phase after standard aging (538 °C/8 h) was determined to be 33%. High-temperature re-solutioning at 927 °C/1 h and subsequent aging at 538 °C/8 h decreased the amount of α precipitate to 24%. Furnace cooling, from 927 °C to room temperature, produced only 14% of α phase, and a subsequent aging heat treatment was necessary to fully harden the material. Furnace cooling from 927 to 538 °C (followed by air cooling to room temperature) and subsequent aging at 538 °C/8 h produced 7.7 and 25% α, respectively.

To ensure hardening of the alloy after aluminum brazing at 677 °C and furnace cooling to 482 °C, the material was aged to produce precipitation of 25% α. Heat treating the as-received alloy at 677 °C/1 h showed no α precipitation, although metallographic evidence (see Fig. 5a below) revealed the presence of the phase.

3.2 *Microstructure of the As-Received Material*

The as-received material consisted of equiaxed β grains, with some areas showing evidence of a nonrecrystallized structure (Fig. 1). Precipitates were observed on grain boundaries and especially on triple grain junctions (Fig. 2). Results of EDS showed that the precipitates were a titanium-rich phase with addition of 9% Mo (Table 4). The phase was suspected to be α-titanium; however, its low aluminum content (<0.4%) precluded this possibility. Other methods, such as transmission electron microscopy/selected-area diffraction (TEM/SAD) need to be employed to identify this phase.

3.3 *Microstructure after Aging of the As-Received Material*

The as-received material (solution treated at 816 °C) was aged at 400 to 677 °C for the times shown in Table 2. At low temperatures (400 °C), precipitation of the α phase occurred in the center of the grains after 4 h (Fig. 3a) and gradually progressed toward the grain boundaries after an aging time of 8 h (Fig. 3b). The precipitates formed at this temperature were too fine to be resolved by SEM. Aging at 538 °C for 8 h resulted in a uniform precipitation of the α phase (Fig. 4). After aging at 677 °C for 1 h, precipitation occurred mainly on the grain boundaries (Fig. 5a) and became more uniformly distributed throughout the grains after aging for 4 h (Fig. 5b). After 8 h at 677 °C (Fig. 5c), no increase in the amount of the α phase was observed, indicating saturation of precipitation at this temperature.

Table 4 Chemical compositions of β matrix and grain-boundary precipitate

	Composition, wt%					
Area	Al	Mo	Si	Nb	Fe	Ti
β matrix	3.20	16.54	0.29	3.18	0.36	bal
Grain-boundary precipitate	0.41	9.20	0	0	0	bal

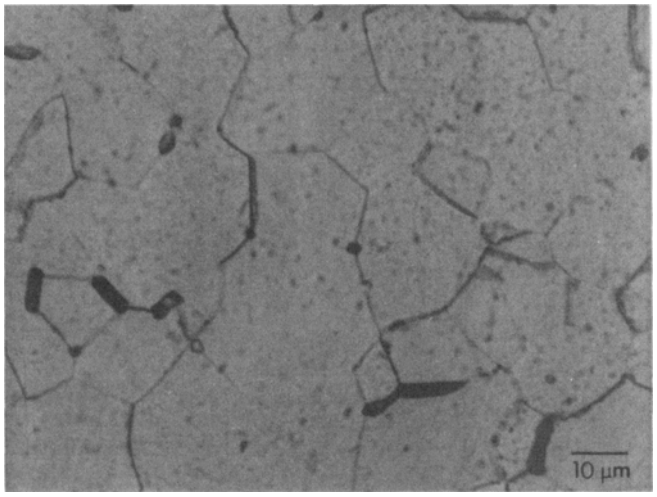

(a)

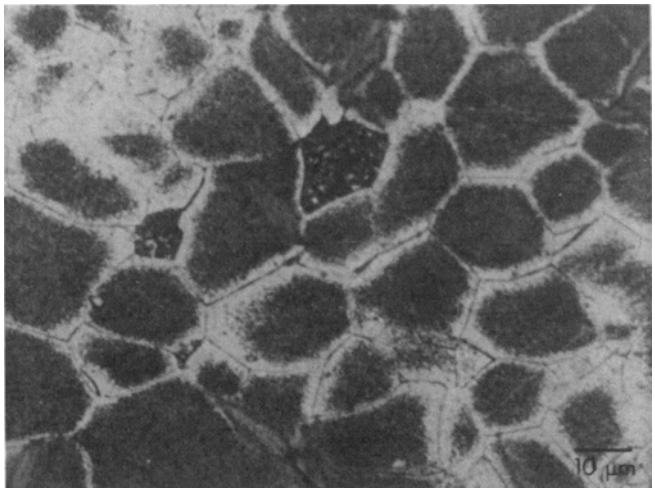

(b)

Fig. 3 Microstructure after aging at 400 °C for (a) 4 h and (b) 8 h

The morphology of the α precipitate was shown by SEM to be acicular in nature and possibly orientated with the matrix. Transmission electron microscopy would be required to identify the nature of the orientation relationship.

3.4 *Effect of Re-Solution Treatment/Aging*

The as-received material was re-solutioned at 816 °C for 1 h, air cooled, and aged at 538 °C for 8 h, resulting in a fine, uniform precipitate of α (Fig. 6). Re-solutioning at 927 °C for 1 h and air cooling resulted in dissolution of grain-boundary precipitate remaining from the as-received microstructure (Fig. 7a). In addition, grain growth increased from the as-received value of 10 μm to 20 and 60 μm after re-solution at 816 and 927 °C, respectively. Subsequent aging at 538 °C for 8 h produced finer α precipitate (Fig. 7b) than the conditions illustrated by Fig. 4, 6, and 7(a).

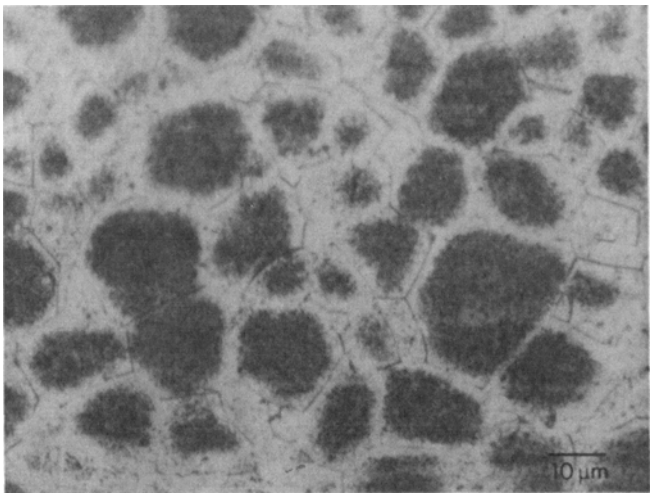

Fig. 2 Microstructure of as-received material showing the grain-boundary precipitate

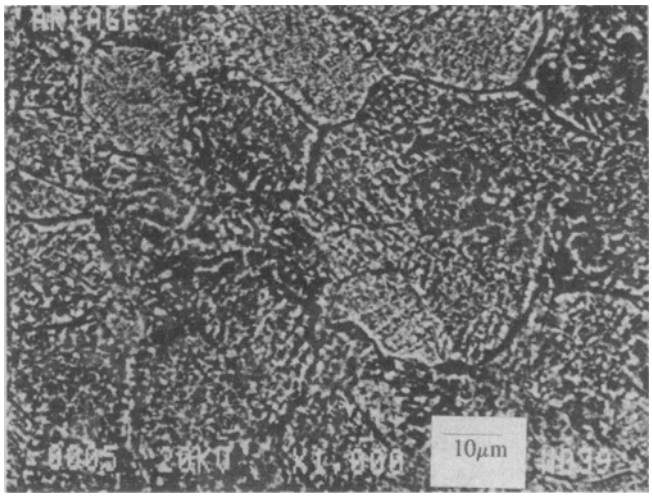

Fig. 4 Microstructure after aging at 538 °C for 8 h

3.5 *Effect of Cooling Rate*

Air cooling at about 22 °C/min from 927 °C (Fig. 7a) suppressed the α precipitation, whereas furnace cooling at 2 °C/min provided sufficient time for α to precipitate. Figures 8(a) to (c) show the sequence of α precipitation during cooling to 593 °C, 538 °C, and room temperature, respectively. During furnace cooling, the α phase formed homogeneously on the grain boundaries and within the grains.

3.6 *Brazing Process*

Titanium brazed with aluminum foil (ABTi) is a thermal cycle that consists of heating to brazing temperature (665 to 680 °C), holding for a time dependent on the part configuration, and furnace cooling at 6 °C/min to below 482 °C before argon quenching to room temperature. A network of α-titanium was produced around the grain boundary as a result of this thermal

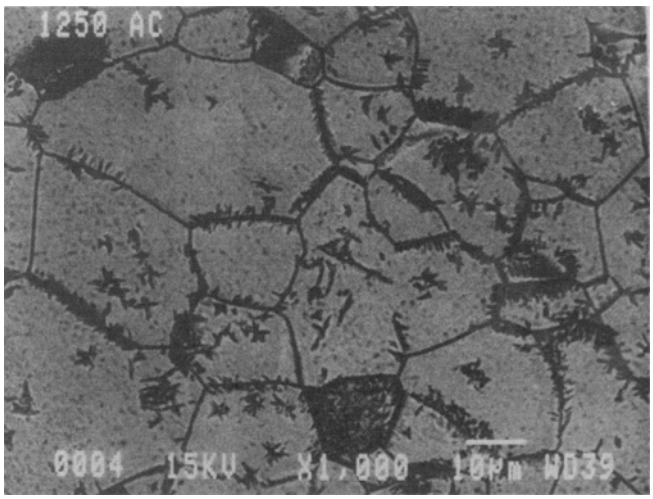

(a)

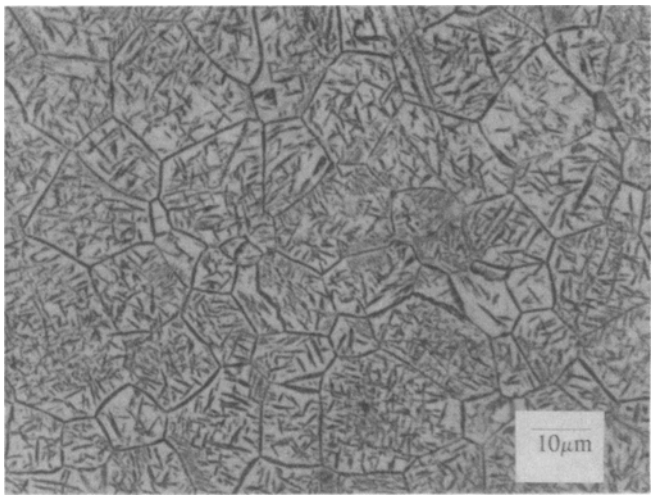

(b)

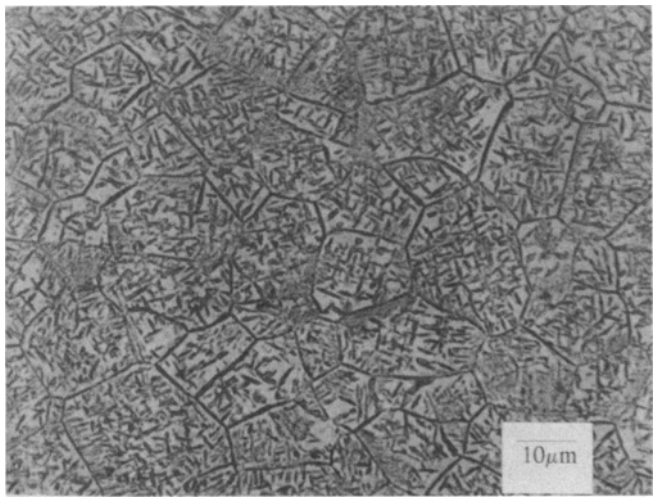

(c)

Fig. 5 Microstructure after aging at 677 °C for (a) 1 h, (b) 4 h, and (c) 8 h

cycle (Fig. 9a); precipitation within the grain was not observed. Subsequent aging after brazing was necessary to bring the material to the hardened condition with 25% of the α phase being precipitated (Fig. 9b).

4. Discussion

4.1 *Effect of Solution Heat Treatment and Cooling Rate*

Varying the solution treatment temperature from the as-received condition (816 °C) to re-solution treatment conditions at 816 and 927 °C increased the grain size from 10 μm to 20 and 60 μm, respectively. Comparing the two extremes (as received and solution treated at 927 °C), it can be seen that the as-received material (Fig. 2) showed grain-boundary precipitates, whereas the 927 °C solution-treated microstructure (Fig. 7a) exhibited no precipitate on grain boundaries. Solution of this grain-boundary phase at the higher temperature (927 °C) removed any inhibition to grain growth, as demonstrated by the increase in grain size.

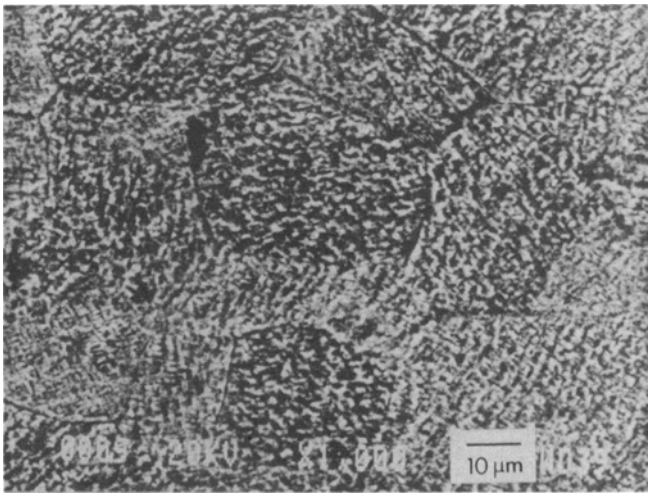

Fig. 6 Microstructure after solution treating at 815 °C for 1 h and at 538 °C for 8 h

Precipitation of the α phase during cooling from 927 °C is influenced by cooling rate and temperature. Air cooling at 22 °C/min (Fig. 7a) resulted in the absence of α phase, whereas furnace cooling at about 2 °C/min resulted in 13.5% α upon cooling to room temperature.

The fine α precipitates that form within the grains during aging after the high-temperature solution treatment have been observed in Ti-15-3, and a theory regarding this has been proposed (Ref 6, 7). Most precipitation reactions take place on defect sites, such as grain boundaries (including interface boundaries), dislocations, and point defects (including vacancies). In this study, it was found that when aging at 538 °C, α tended to precipitate uniformly within grains; it is likely that the nucleation sites were vacancies. Higher solution temperatures give rise to an increased vacancy concentration, and higher quenched-in vacancies after air cooling, which supplies more precipitation sites.

The relationship between vacancy concentration (C_v) and solution temperature can be expressed as:

$$C_v = A_{exp}\left(\frac{-Q}{kT}\right)$$

where Q is the vacancy formation energy (Ref 8), A is the geometry factor, k is Boltzmann's constant, and T is temperature in degrees Kelvin. It can be seen that as the solution temperature increases, the equilibrium vacancy concentration increases. When a relatively fast cooling rate is used (water quenching or air cooling), there will not be enough time for all vacancies to be annihilated in the available vacancy sinks, and an excess of vacancies will remain after cooling to room temperature. This would account for the uniform distribution of fine α precipitation observed from aging at 538 °C after high-temperature solutioning.

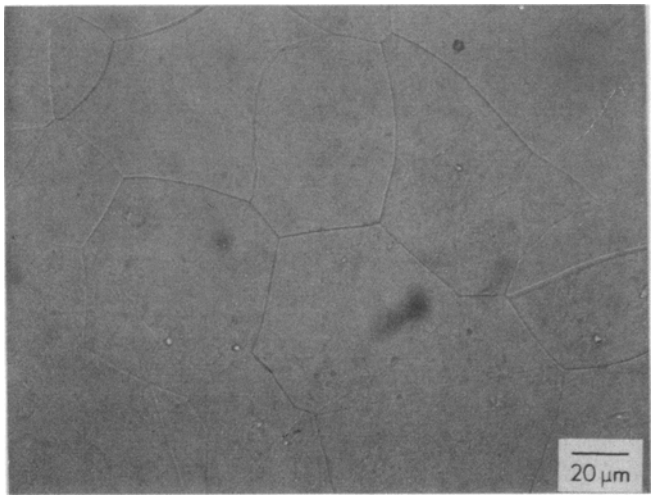

(a)

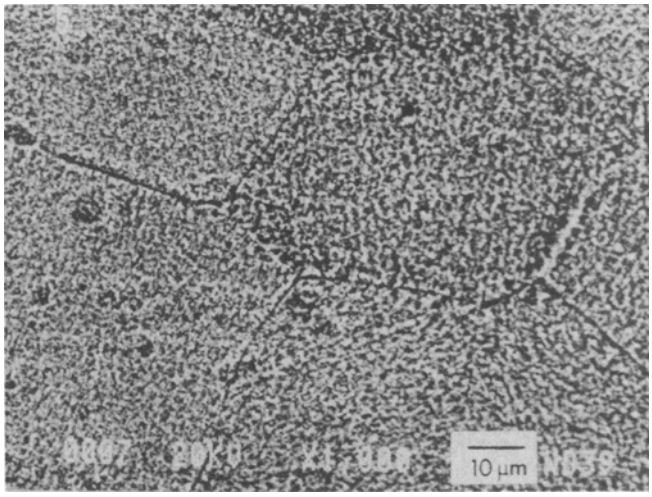

(b)

Fig. 7 Microstructure after solution treating (a) at 927 °C for 1 h and (b) at 927 °C for 1 h, followed by aging at 538 °C for 8 h

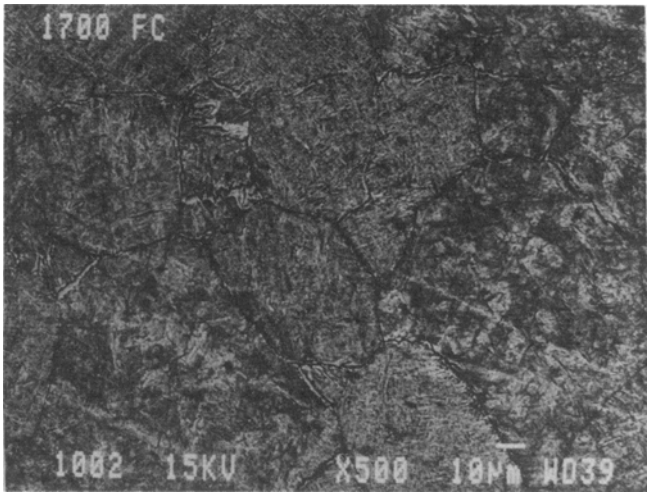

(a)

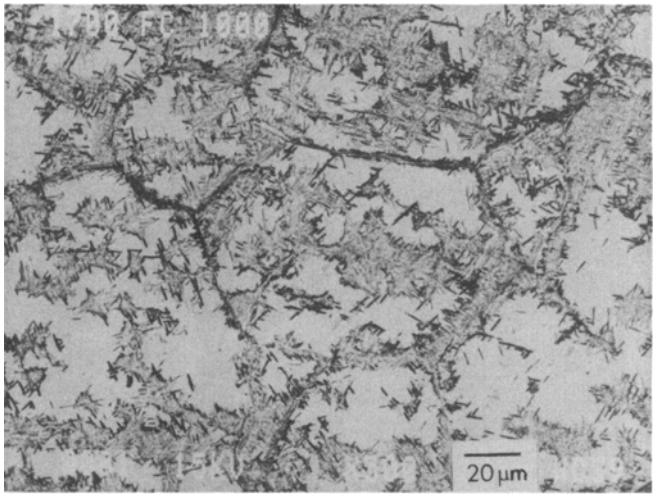

(b)

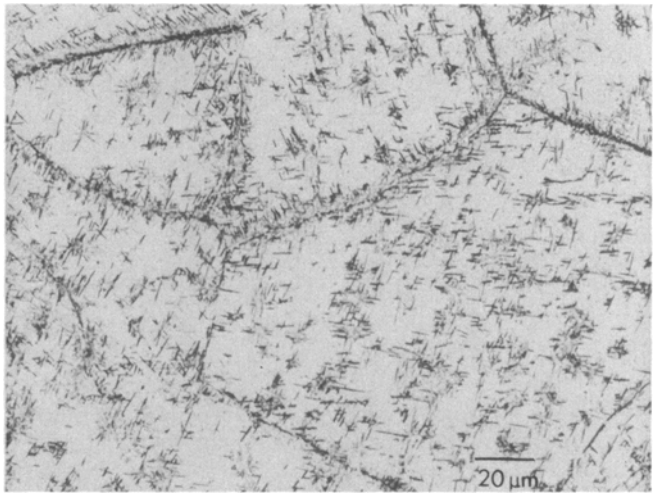

(c)

Fig. 8 Microstructure after solution treating at 927 °C for 1 h, followed by furnace cooling to (a) 593 °C, (b) 538 °C, and (c) room temperature

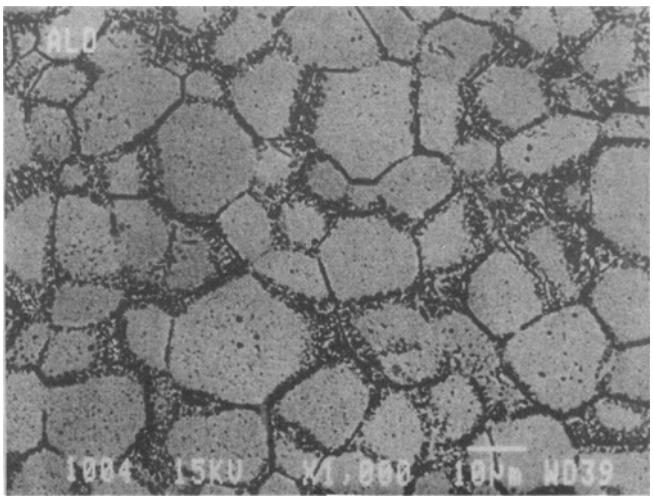

(a)

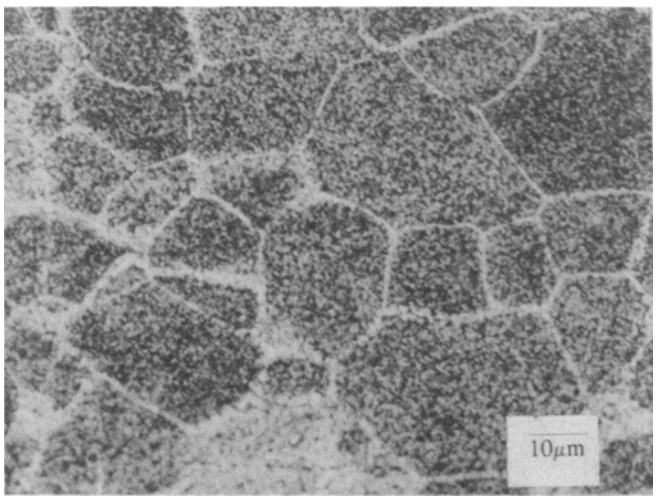

(b)

Fig. 9 Microstructure after (a) ABTi cycle and (b) ABTi cycle, followed by aging at 538 °C

4.2 *Effect of Aging Temperature and Time*

Differences in α precipitation behavior were readily discerned from the aging cycles. At low aging temperatures (400 °C), precipitation initiated within the grains and progressed closer to the grain boundaries as time increased; in addition, a precipitate-free zone was observed near the grain boundaries at the low aging temperature (Fig. 3a and b). Aging at 538 and 677 °C resulted in the formation of α initially on grain boundaries (Fig. 4 and 5) and then within the grains. The precipitate size increased with increasing aging temperature, whereas the amount of precipitate increased with increasing aging time at a constant temperature until saturation occurred.

A possible mechanism for this phenomenon is as follows. At low aging temperature, α-titanium prefers to precipitate on vacancies if possible. An excess vacancy concentration is produced by solution treatment and fast (air) cooling, as previously described. At the same time, vacancies move toward vacancy sinks (grain boundaries in this case) during aging. Therefore, areas near the grain boundaries have a lower vacancy density than the center of the grain, which causes a precipitation depletion zone when aging at high temperature (677 °C). The excess vacancy concentration is reduced by annihilation at vacancy sinks. This lessens the importance of vacancies on precipitate distribution and causes grain boundaries to become a more dominant site for α precipitation during the initial stages of aging. The formation energies of α both on vacancies and on grain boundaries may also affect the precipitation distribution.

5. Conclusions

High-temperature solution heat treatment (927 °C) produced finer α precipitates during aging, which may be attributed to a larger amount of quenched-in vacancies.

Alpha precipitated within the grains at low aging temperatures (400 °C), leaving a precipitate-free zone adjacent to the grain boundaries. The α precipitates were much smaller in size compared to those formed at a higher aging temperature.

The precipitation of α phase began mainly on grain boundaries when aging at higher temperatures (such as 677 °C), due to a lower vacancy concentration.

Cooling rate from solution temperature influenced α precipitation. Air cooling resulted in suppression of precipitation, whereas furnace cooling ensured sufficient time to precipitate the phase. Aging was necessary to ensure an α content greater than 20%.

Acknowledgment

Special thanks are due to Mr. N. Ball, Department of Geological Sciences, University of Manitoba, for conducting the XRD experiments.

References

1. P.J. Bania and W.M. Parris, paper presented at TDA International Conference (Orlando, FL), 1990
2. T.A. Wallace, R.K. Clark, and K.E. Wiedemann, NASA Tech. Memo. 104217, NASA Langley Research Center, Hampton, VA, March 1992
3. J.S. Grauman, paper presented at TDA International Conference (Orlando, FL), 1990
4. K.E. Wiedemann, R.K. Bird, T.A. Wallace, and R.K. Clark, NASA Tech. Memo. 104220, NASA Langley Research Center, Hampton, VA, June 1992
5. R.J. Hill and C.J. Howard, *J. Appl. Crystallogr.*, Vol 20, 1987, p 467-474
6. H. Fuji and H.G. Suzuki, *J. Jpn. Inst. Met.*, Vol 55 (No. 10), 1991, p 1063-1070
7. T. Kurado, I. Horinouchi, O. Iwagi, K. Morl, and F. Matsuda, *Trans. JWRI*, Vol 19 (No. 1), 1990, p 79-86
8. P. Doig and P.E. Flewitt, *Acta Metall.*, Vol 29, 1981, p 1831-1842